ORGANIC CHEMISTRY FRONTIERS

RESEARCH ARTICLE

View Article Online
View Journal | View Issue



Cite this: *Org. Chem. Front.*, 2025, **12**, 2676

# Successive energy-transfer catalytic dearomative reactions of quinolines with bicyclo[1.1.0]butanes for the synthesis of pyridine-fused 3D complicated molecules†

Yi-Ping Cai, Shi-Ru Chen and Qin-Hua Song *

Dearomative photocycloadditions are unique and hard to replace methods for the construction of various polycyclic strained molecules to increase saturation and create three-dimensional (3D) molecular complexity. In this article, we report a facile photochemical strategy for the synthesis of pyridine-fused 3D polycyclic molecules from quinolines and bicyclo[1.1.0]butanes (BCBs) under visible-light conditions. The dearomative reactions proceed *via* an initial triplet–triplet energy transfer (EnT) enabled [2π + 2σ] cycloaddition to form an adduct, in which the vinylpyridine moiety is still excitable under the same photosensitive conditions. By introducing a suitable alkyl group as an H-donor into a BCB, a 1,6-hydrogen atom transfer (HAT) would occur from the alkyl group to the excited vinylpyridine moiety *via* a second EnT process, generating a 1,7-diradical; subsequent ring closure produces a seven-membered 2D/3D-fused molecule. The rare 1,6-HAT process was confirmed through dynamic tracking, control experiments, quenching studies and deuterium-labeling experiments. Applying this strategy, we have successfully obtained a series of structurally unique 6-6-5-4-7 ring 3D molecules with wide functional group tolerance and compatibility with various C–H bonds and various quinolines. Meanwhile, it provides a new idea for the construction of polycyclic architectures by utilizing the infrequent 1,6-HAT of an excited olefin to generate 1,7-diradical species.

Received 29th January 2025,
Accepted 19th February 2025

DOI: 10.1039/d5qo00205b

rsc.li/frontiers-organic



## 1. Introduction

Polycyclic architectures are frequently found in drugs and bioactive natural products, some of which are important pharmacodynamic carriers.[1] Two-dimensional (2D) aromatic rings such as pyridine and benzene are the most common scaffolds, followed by three-dimensional (3D) aliphatic groups ranging from 3- to 6- or even 7-membered rings.[2] Owing to their unique structural and physicochemical properties, the 3D aliphatic rings have gained more and more attention in drug discovery, for example, some natural products with 7-membered rings exhibit significant pharmacodynamic activity (Scheme 1a).[3] For example, salimabromide originating from marine myxobacteria is a potential inhibitor of *Arthrobacter crystallopoietes*.[3a] For this reason, the methodologies for constructing fused 2D/3D ring molecular architectures have attracted increasing research interest over the past few decades, especially after the concept of "escape from flatland" was proposed in medicinal chemistry.[4]

Dearomative photocycloaddition (DAPCA) is an effective approach for increasing the saturation of aromatic materials by forming bridging C($sp^3$)–C($sp^3$) bonds on the aromatic ring with excellent step/atom economy.[5] Arenes in the excited state add to the carbon–carbon double bond of a wide variety of alkenes by three modes, 1,2(*ortho*), 1,3(*meta*) or 1,4(*para*) cycloaddition. The 1,3(*meta*) mode is the only one to be allowed as a concerted pericyclic reaction, and the 1,2(*ortho*) and 1,4 (*para*) modes proceed *via* a stepwise pathway of the triplet excited state.[6] The long-lived triplet excited states of arenes enable intermolecular cycloadditions to occur.[7] Owing to the inherent chemo- and regioselectivity toward intermolecular DAPCA reactions, the multifaceted chemistry of the photocycloadducts provides a valuable pathway for constructing various complicated carbon frameworks, which would be difficult to synthesize *via* other routes.[8]

Photosensitization, *via* triplet–triplet energy transfer (EnT) in the presence of a triplet photosensitizer (or a photocatalyst),

*Department of Chemistry, University of Science and Technology of China, Hefei 230026, P. R. China*

†Electronic supplementary information (ESI) available: Experimental procedures, characterization data of related compounds, mechanistic studies, X-ray crystal structure data and NMR spectra. CCDC 2382179 (for *cis*-**4A**), 2382180 (for *trans*-**4A**), 2382181 (for *cis*-**4f**), 2382182 (for *cis*-**4h**), 2382183 (for *trans*-**4n**) and 2382185 (for *cis*-**4wd**). For ESI and crystallographic data in CIF or other electronic format see DOI: **https://doi.org/10.1039/d5qo00205b**

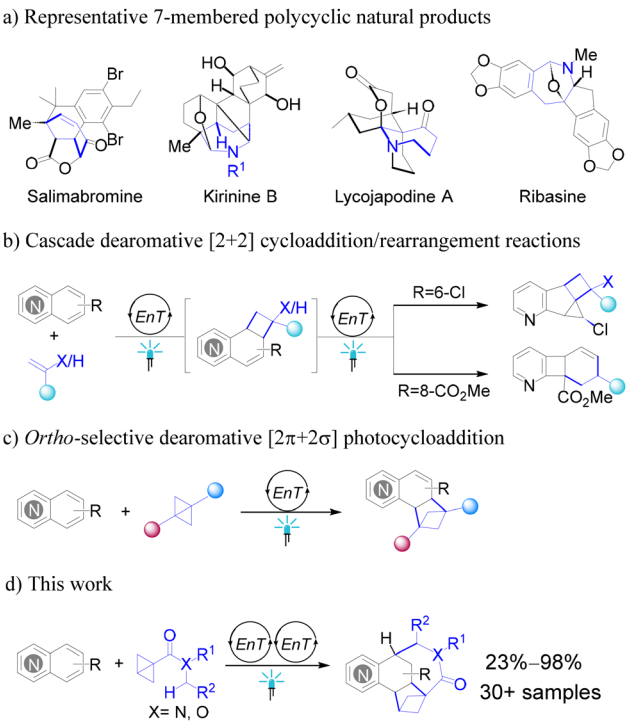


**Scheme 1** Background and our proposal.

is one of the important photochemical activation modes in synthetic chemistry. Recently, using a metal complex [Ir–F] as a photocatalyst, Glorius and coworkers, in collaboration with Brown's and Houk's groups, have successfully achieved the EnT-enabled dearomative *para*-[4 + 2] cycloaddition of N-heteroarenes, selectively saturating the benzenoid rings.[9] Subsequently, they reported two types of highly efficient and selective intermolecular cascade dearomative *ortho* (5,6- or 7,8-) [2 + 2] cycloaddition/rearrangement reactions of quinoline derivatives with alkenes. These reactions commence with the first EnT-enabled [2 + 2] cycloaddition of quinolines, with chloro or ester substitutions at the benzenoid rings, followed by a second EnT-enabled either cyclopropanation or cyclobutane rearrangement (Scheme 1b).[10] The initial EnT-mediated adducts contain a strained four-membered ring and an excitable vinylpyridine moiety, whose photolability consequently limits their synthetic accessibility. For this reason, Glorius, Houk and coworkers proposed a strain-release approach[11] as a thermodynamic strategy to conserve the original *ortho*-adduct by forming cycloaddition products. Using bicyclo[1.1.0]butanes (BCBs) instead of alkenes as 2σ-electron partners, they achieved the dearomative [2π + 2σ] photocycloaddition of bicyclic aza-arenes to enable direct construction of *ortho*-cycloaddition products with a blocked tendency to undergo downstream rearrangements or cycloreversion (Scheme 1c).[12] A series of stable *ortho*-selective [2π + 2σ] cycloadducts were obtained in this excellent work; however, the photoactive vinylpyridine moieties still remain. We questioned whether these moieties could be excited *via* a second EnT process to trigger new reactions such as dimerization and intramolecular or intermolecular [2 + 2] cycloaddition with other olefin partners.

Carbon-to-carbon intramolecular 1,*n*-HAT (*n* = 5, 6) processes occur in excited triplet olefins *via* a visible-light EnT process. These reactions have been used by multiple research groups to construct specific (*n* − 1)-membered rings.[13] Inspired by this, we propose the following hypothesis: if an appropriate substituent is introduced into a BCB, the excited triplet vinylpyridine moiety of the first EnT-mediated [2π + 2σ] cycloadduct could undergo a 2nd EnT process, abstracting a hydrogen atom from the substituent *via* a HAT process to generate a diradical, which subsequently couples to afford a cyclic product. In this article, we have realized this idea, that is, we developed a facile synthetic strategy for producing pyridine-fused polycyclic 3D molecules with high structural complexity *via* successive EnT-mediated dearomative reactions in simple photochemical systems under mild metal-free catalytic conditions (Scheme 1d).

## 2. Results and discussion

### Reaction optimization

Selecting unsubstituted quinoline **1a** and the BCB *N*,*N*′-dibenzylbicyclo[1.1.0]butane-1-carboxamide (**2a**) as starting materials, we performed a model reaction in the presence of thio-

**Table 1** Reaction optimization and control experiments[a]

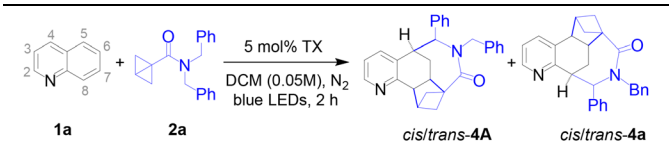


| Entry | Deviation[b] | Yield/% | rr | dr |
|---|---|---|---|---|
| 1 | None | 92 | 3.5 : 1 | 1.4 : 1 |
| 2 | [Ir–F][c] (60.9) instead of TX (65.5) | 49 | 3.6 : 1 | 1.5 : 1 |
| 3 | 3-MeOTX (67.6) instead of TX | 26 | 4.2 : 1 | 1.4 : 1 |
| 4 | 3-FTX (67.4) instead of TX | 70 | 4.2 : 1 | 1.4 : 1 |
| 5 | 2-iPrTX (63.6) instead of TX | 71 | 3.4 : 1 | 1.4 : 1 |
| 6 | 2-MeOTX (57.8) instead of TX | Trace | — | — |
| 7 | 2,2′-MeOTX (55.2) instead of TX | n.d. | — | — |
| 8 | Adding 1.25 equiv. *p*-TsOH | 19 | 4.4 : 1 | 1.0 : 1 |
| 9 | $CHCl_3$ instead of DCM | 71 | 3.7 : 1 | 1.5 : 1 |
| 10 | Kessil LED (427 nm) | 41/60[d] | 3.9 : 1 | 1.3 : 1 |
| 11 | Under air | 42 | 4.4 : 1 | 1.5 : 1 |
| 12 | Under an $O_2$ atmosphere | 9 | — | 1.2 : 1 |
| 13 | In the dark | n.d. | — | — |
| 14 | No PC | n.d. | — | — |

[a] Standard conditions: **1a** (0.1 mmol, 1.0 equiv.), **2a** (2.0 equiv.), thioxanthone (TX, 5 mol%), DCM (0.05 M), $N_2$, and blue LED ($\lambda_{max}$ = 400 nm) for 2 h, unless otherwise stated. Reported yields are from $^1$H NMR total yields of all regioisomers (**4A**/**4a**, rr) or all diastereoisomers. The diastereomeric ratio (dr) is given as the ratio of *cis*-**4A**/*trans*-**4A**, which is defined by the relative position between 5-H (8-H for **4a**) and H at methine of benzyl (for details see the ESI†); n.d., not detected. [b] Triplet energies $E_T$ (kcal mol$^{-1}$) in parentheses from ref. 15. [c] 2 mol% [Ir–F], LED (450–460 nm). [d] For 5 h.

xanthone (TX) as a triplet photosensitizer under visible-light irradiation (Table 1; for details, see the ESI†). The photochemical reaction of unsubstituted quinoline **1a** with the BCB generates two comparable regioisomers (from the 8-to-7 adduct/5-to-6 adduct, rr 3.5 : 1) in a high yield (92%). The whole process seems to be the [2π + 2σ] cycloaddition *via* the first EnT process, and the *N*,*N*′-dibenzyl moiety from **2a** can act as an HAT-donor in the second EnT, and cyclization after the HAT process produces transannular products, featuring a structurally unique pyridine-fused 6-6-5-4-7 ring system, in which **4A** is the major regioisomer (derived from the 8-to-7 adduct) with a low diastereoselectivity (dr 1.4 : 1). Their constitutions and relative configurations were tentatively assigned based on NMR and later unequivocally corroborated by single-crystal X-ray crystallography.[14] Our initial idea was to perform this reaction under a variety of conditions to find the conditions that would achieve the reaction with high regioselectivity and high diastereoselectivity.

Using [Ir–F] as a photosensitizer and $Sc(OTf)_3$ as an additive, Glorius, Houk and coworkers reported the formation of a [2π + 2σ] *ortho*-adduct in a high yield of 92% from a photochemical system, comprising 7-methoxyquinoline and a BCB in a molar ratio of 2 : 1.[12] To compare with this result, we evaluated the efficiency of the system by replacing TX with [Ir–F] as the photosensitizer, and obtained a low yield of 49% (entry 2). Further examination of a series of thioxanthones (TXs) with various triplet energies indicated that TX affords the highest yield of 92% within a short irradiation time of 2 h.

The triplet energy ($E_T$) of quinoline is about 61.7 kcal $mol^{-1}$,[9a] 65.5 kcal $mol^{-1}$ for TX and 60.9 kcal $mol^{-1}$ for [Ir–F].[15] The modification of TX can adjust its triplet energy level. For example, a 2-substituted TX has a lower $E_T$ and a longer absorption band, while a 3-substituted one is the opposite.[15] For various TXs in the order of decreasing triplet energy, the yield rises first and then falls rapidly, from 3-MeOTX (26%) to 3-FTX (70%), then 2-iPrTX (71%), and 2-MeOTX (trace) to 2,2′-MeOTX (n.d.) (entries 3–7). The low yield of 3-MeOTX may be due to its short absorption band leading to weaker absorption of the blue LED, and that of 2-MeOTX and 2,2′-MeOTX are due to their lower triplet energies than that of quinoline, preventing them from facilitating the EnT process.

Based on previous reports,[9,12,16] we attempted to add *p*-TsOH to our system to decrease the triplet energy of **1a** for elevating the reaction efficiency. However, a lower yield of 19% and loss of diastereoselectivity were obtained (entry 8). Additionally, using chloroform as the solvent led to a notable decrease in the reaction efficiency (entry 9). The above results were compared with those obtained using a familiar light source, a Kessil LED (427 nm), and a yield of only 41% was obtained under irradiation with this lamp, and up to 60% after an additional 3 h of irradiation (entry 10). The reaction without degassing could also provide a yield of 42% (entry 11), while under an $O_2$ atmosphere, this reaction was significantly suppressed, giving an extremely low yield of 9% (entry 12). Finally, no desired product was observed in the dark (entry 13) or in the absence of the photocatalyst (entry 14). The results disclose the coerciveness of both visible light and the photosensitizer for this transformation.

### Reaction scope

With the optimized conditions identified, we next investigated the substrate scope of our protocol. First, **2a** with *N*,*N*′-dibenzyl was used as the limiting reagent, reacting with various substituted quinolines (the preparation details are provided in the ESI†). Quinolines bearing 2-, 3-, or 4-methyl groups at the pyridine moiety transformed into the desired products in yields of 76%–98%, which were formed mainly from 8-to-7 *ortho*-adducts, and the *cis*-isomers were typically obtained in modest excess. Thus, the methyl group at the pyridine ring has a slight effect on both regioselectivity and diastereoselectivity. However, for 5-, 6-, 7-, or 8-methyl groups at the benzenoid ring of quinolines, a notable regioselectivity of the [2π + 2σ] cycloaddition was observed and the results are shown in Table 2. For 5- or 7-methyl quinolines, 8-to-7 cycloadducts are the major regioisomers (**4E**, **4G**), while regioselective 5-to-6 adducts are the major regioisomers for 6- or 8-substituted quinolines (**4f**, **4h**). The structures of *cis*-**4f** and *cis*-**4h** have been unequivocally assigned based on their crystal X-ray crystallographic data.[14]

As quinoline is excited to its triplet state by EnT from the excited triplet TX, its 5- or/and 8-carbon with a high electron density nucleophilically attacks a BCB, forming a 5-diradical (5-Int-1) or/and an 8-diradical (8-Int-1), respectively.[9b] The formation and stability of two diradicals could be critical for the regioselectivity (Fig. 1). The methyl at the 6- or 7-position can stabilize the diradical intermediate 5-Int-1 or 8-Int-1, respectively, and 5- or 8-methyl groups could introduce steric hindrance for the nucleophilic addition of the excited quinoline to a BCB. Thus, combining the two factors, the major regioisomers are derived from 5-to-6 adducts for the methyl group at the 6- or 8-position, and from 8-to-7 adducts for the methyl group at the 5- or 7-position. Besides high regioselectivity, 5- and 8-methyl quinolines displayed high diastereoselectivity (dr 5.3 : 1 for **4E**, 8.1 : 1 for **4h**) and low values for others (dr 1.5 : 1 for **4f** and **4G**).

For 5,7-dimethyl quinoline, the combined effects, *i.e.* 5-methyl blocking the formation of 5-Int-1 and 7-methyl stabilizing 8-Int-1, lead to the formation of the regiospecific [2 + 2] cycloadduct (from 8-Int-1) **3I** (untransformed 34%) and the corresponding final product **4I** in a yield of 10%. This implies a low efficiency of the second EnT-mediated HAT process, possibly due to the steric hindrance of the two methyl groups in **3I**. It is worth noting that the diastereospecificity (dr >19 : 1, only *cis*-**4I**) could be due to the steric effects of the 5,7-dimethyl group (*vs.* **4E** (5.3 : 1), **4G** (1.5 : 1), and **4A** (1.4 : 1)). Similar to methyl, both 4-Ph and 4-Br quinolines convert well to the desired products with 66% and 63% yields, respectively, in which the former has a better rr value of 7.3 : 1 than 4-Me quinoline (3.9 : 1). A reverse diastereoselectivity was observed in the 4-Br quinoline system, that is, the *trans*-diastereomer became predominant (*cis*-/*trans*-**4K**, 1 : 2.1 *vs.* **4J**, 1.4 : 1).

 

**Table 2** The scope of quinolines and structures of major target products[a]

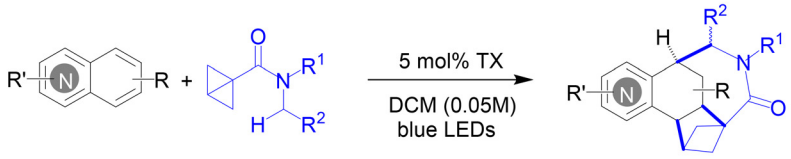


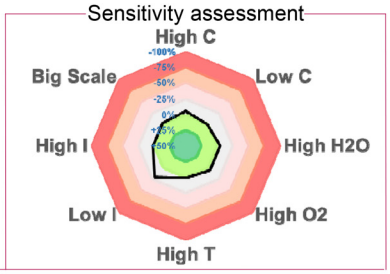


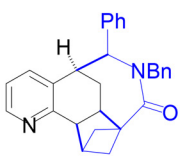


**4A**, 92%
3.5:1 r.r., 1.4:1 d.r.

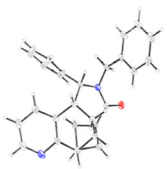

[X-ray] *cis*-**4A**

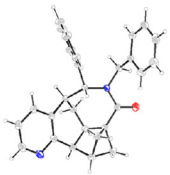

[X-ray] *trans*-**4A**

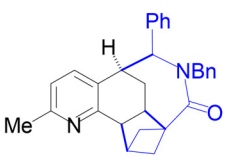


**4B**, 97%
2.7:1 r.r., 1.5:1 d.r.

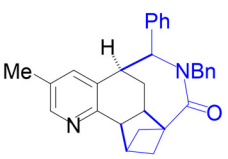


**4C**, 76%
3.8:1 r.r., 1.5:1 d.r.

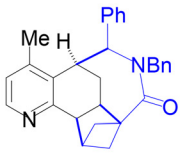


**4D**, 98%
3.9:1 r.r., 1.4:1 d.r.

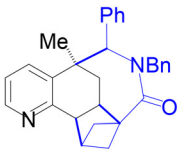


**4E**, 81%
13.0:1 r.r., 5.3:1 d.r.

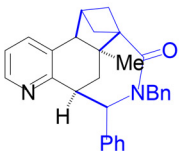


**4f**, 80%
2.3:1 r.r., 1.5:1 d.r.

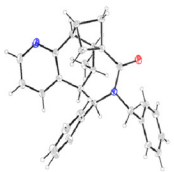

[X-ray] *cis*-**4f**

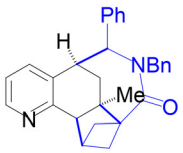


**4G**, 57%
10.4:1 r.r., 1.5:1 d.r.

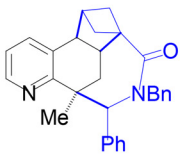


**4h**, 61%
2.8:1 r.r., 8.1:1 d.r.

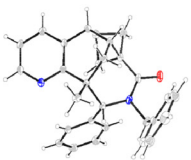

[X-ray] *cis*-**4h**

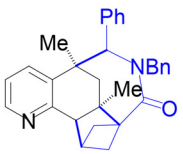


**4l**,10%(34%**3l**)[b]
>19:1 r.r., >19:1 d.r.

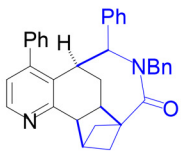


**4J**, 66%
7.3:1 r.r., 1.4:1 d.r.

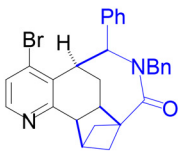


**4K**, 63%
2.2:1 r.r., 1:2.1 d.r.

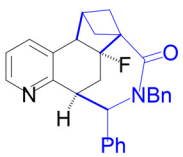


**4l**, 66%
1.1:1 r.r., 1.2:1 d.r.

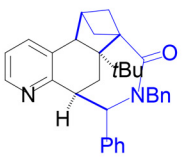


**4m**, 85%
>19:1 r.r., 2.9:1 d.r.

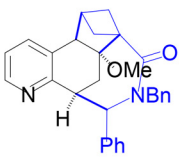


**4n**, 55%
>19:1 r.r., 1.0:1 d.r.

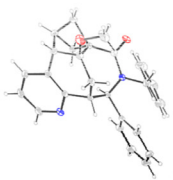

[X-ray] *trans*-**4n**

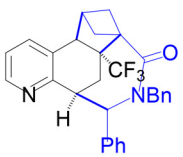


**4o**, 78%
>19:1 r.r., 1.2:1 d.r.

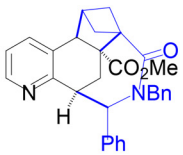


**4p**, 23%[c]
>19:1 r.r., 2.3:1 d.r.

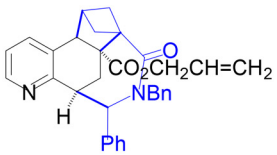


**4q**, 25%[c]
>19:1 r.r., 1.5:1 d.r.

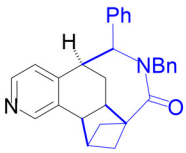


**4R**, 52%[c]
>19:1 r.r., 2.1:1 d.r.

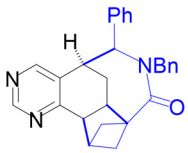


**4S**, 70%
7.8:1 r.r., 1.1:1 d.r.

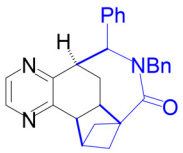


**4T**, 68%
1:1.1 d.r.

[a] Reaction conditions: **1** (0.2 mmol, 1.0 equiv.)), **2** (2.0 equiv.) and TX (5 mol%) in DCM (0.05 M), $N_2$ and blue LEDs ($\lambda_{max}$ = 400 nm) for 2–26 h, unless otherwise stated. Owing to some minor isomers not being isolated, the yields are $^1$H NMR yields of all isomers, and only the structures of the major regioisomers are shown, using capital letters for products from 8-to-7 adducts such as **4A** and lowercase letters for 5-to-6 adducts such as **4a**; and isolated yields are provided in the ESI.† The values of rr and dr were obtained from $^1$H NMR analysis of the crude product mixture. The dr values (*cis* : *trans* ratio) refer to the major regioisomers. [b] *ortho*-Cycloadduct. [c] 2% [Ir–F], HFIP (0.05 M), blue LED (450–460 nm).

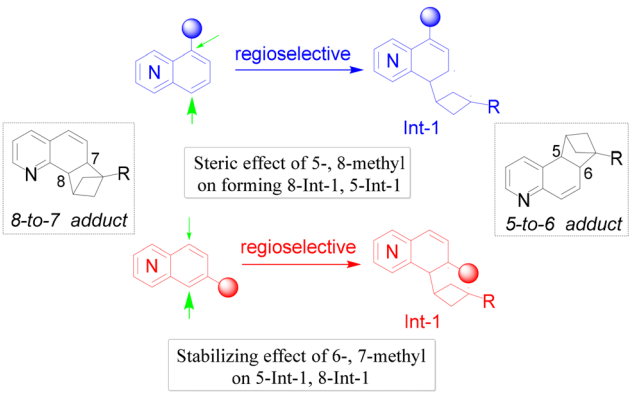


**Fig. 1** Substituent effects on the regioselectivity of 8-to-7 *vs.* 5-to-6 adducts.

Similar to 6-methyl, a single 6-F atom also leads to reverse regioselectivity (rr **4L**/**4l** 1 : 1.1 *vs.* **4A**/**4a** 3.5 : 1). For larger 6-groups, including 6-*t*Bu, 6-$OCH_3$, 6-$CF_3$, 6-$CO_2Me$ and 6-$CO_2CH_2CH{=}CH_2$, only single regioisomers were observed (**4m**, **4n**, **4o**, **4p** and **4q**), among which the crystal structure of *trans*-**4n** was determined. Both electron-donating (*t*Bu, $OCH_3$) and electron-withdrawing (F-, $CF_3$-, $CO_2Me$, $CO_2CH_2CH{=}CH_2$) groups can well achieve the transformation (55–85%) except for the two carbonyl-containing substituents with low yields (23% for **4p**, 25% for **4q**), possibly greatly affecting the photophysical properties of quinoline. Other aromatic heterocycles, isoquinoline (52%), quinazoline (70%) and quinoxaline (68%), are compatible with our protocol. Among them, isoquinoline is regiospecific (>19 : 1) and highly diastereoselective (2.1 : 1), while quinazoline shows high regioselectivity (7.8 : 1).

After assessing the feasibility of quinolines, we next evaluated their partners BCBs (**2**) (Table 3). First, by replacing the N-atom with an O-atom, a BCB ester also achieved the desired reaction in a moderate yield (**4U**, 43%). Here, *p*-TsOH was added for suppressing hydrolysis of the ester by neutralizing the alkaline pyridine. Replacing the benzyl group in **2a** with one methyl group resulted in **2v**, where a significant decrease in the yield (36%) with improved regioselectivity (8.0 : 1) was observed. When the BCB **2v** was reacted with 6-*t*Bu-quinoline, the desired product **4wa** was obtained in a good yield (74%) with reverse diastereoselectivity (1 : 1.4 *vs.* 1.3 : 1 (**4V**) and 2.9 : 1 (**4m**)). When the methyl group of **2v** is replaced by a phenyl group to form **2w**, a better diastereoselectivity was observed (1 : 2.9 (**4w**) *vs.* 1 : 1.4 (**4wa**)).

Considering its high reactivity and regiospecificity, 6-*t*Bu quinoline was selected as the partner for various BCBs. By varying substituents on the amino group of BCBs with phenyl (Ph), methyl (Me), ethyl (Et), isopropyl (iPr) or *tert*-butyl (*t*Bu) groups, the corresponding products (**4w**–**4wd**) could be obtained in yields ranging from 39% to 74%. It is worth highlighting that the BCB with a large *tert*-butyl group at the amino reacts effectively, converting to *cis*-**4wd** as the sole regioisomer and diastereomer with a yield of 60%. The X-ray crystal structure of *cis*-**4wd** [14] shows that the phenyl group of *N*-benzyl is on another side of 6-*t*Bu and *N*-*t*Bu. Upon replacing the benzyl group with a more electron-rich 4-methoxybenzyl group, a higher diastereoselectivity (**4we**, 3.8 : 1 dr) is obtained relative to that of **4m** (2.9 : 1 dr).

The above 1,6-HAT process occurs only at the methylene of benzyl possibly due to the low C–H bond dissociation energy (BDE) of the methylene (89 kcal $mol^{-1}$).[17] To explore the possibility of a 1,6-HAT process for other alkyl groups (Me, Et, iPr and *t*Bu), we prepared *N*,*N*′-dialkyl substituted BCB amides **2f**, **2g** and **2h**. Under the same conditions, the desired products **4wf**, **4wg** and **4wh** were obtained in yields of 59%, 38% and 25%, respectively. Unexpectedly, the hydrogen of the *N*-Me group rather than that ($Me_2CH$) of the *N*-iPr group is abstracted to generate a single regioisomer **4wh**. The BDEs of the C–H bonds of *N*-Me, methylene of *N*-Et and methine of *N*-iPr are 91,[17] 90.7 [17] and 88.4 [18] kcal $mol^{-1}$, respectively. Obviously, the 1,6-HAT process can occur for the above various C–H bonds. Namely, the BDE of the C–H bond is not a determining factor, but rather the closer spatial distance between the H-acceptor and H-donor. Fouassier *et al.* have observed similar results.[19]

We have had a few unsuccessful cases, and a limited scope of BCBs is available in the ESI.† The BCBs with a methine of iPr and methylbenzyl, or phenyl did not achieve the desired reaction. Combining with the results in Table 3, steric hindrance (or spatial distance) is the main factor for iPr and methylbenzyl, while phenyl may be thermodynamically unfavorable due to its high BDE (113 kcal $mol^{-1}$).

Additionally, a condition-based sensitivity assessment was performed and is shown in Table 2. No significant effect on most parameters (concentration, water and temperature) was observed, but insufficient light intensity and high $O_2$ concentration caused adverse effects. Adequate light intensity is pivotal for the effective operation of the reaction. To our delight, the optimized reaction conditions were highly reproducible at large scales (20-fold optimized scale), asserting the practicability of the present protocol.

## Synthetic applications

To illustrate the synthetic practicability of this protocol, further transformations and derivatizations of the typical products *cis*/*trans*-**4A** were conducted. As exemplified in Scheme 2, the amide moiety was efficiently reduced to the aldehyde product **5** with a secondary amine using $LiAlH_4$ in a yield of 78% (reaction (a)), in which two chiral centers are constructed selectively. Using Lawesson's reagent, the thionation of the carbonyl afforded **6** in 86% yield (reaction (b)). Furthermore, the pharmaceutically relevant pyridine *N*-oxide scaffold **7** can be easily achieved in almost quantitative yield (reaction (c)) through treatment with *m*-CPBA, which might be facilely transformed into C2-functionalized pyridines, thereby highlighting its utility as a versatile tool for downstream diversification.[20] Finally, a C–Br bond was established at the pyridine ring **8** upon treatment with $Br_2$ (reaction (d)). Obviously, this is beneficial for the late-stage functionalization of active pharma-

 

**Table 3** The scope of BCBs and structures of major target products[a]

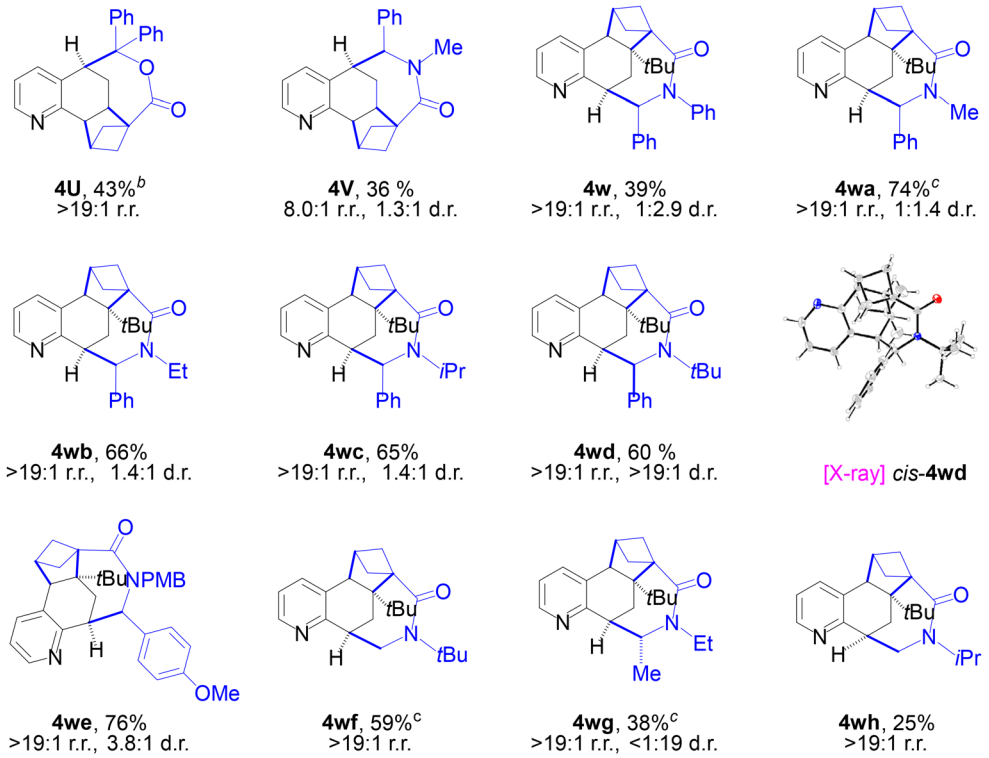


[a] Reaction conditions: see Table 2. [b] 1.25 equiv. *p*-TsOH. [c] 4.0 equiv. BCBs. PMB: *p*-methoxybenzyl.

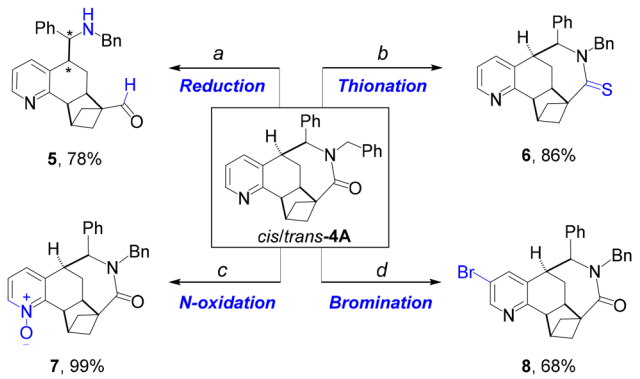


**Scheme 2** Synthetic applications. Reagents and conditions: (a) $LiAlH_4$ (4.0 equiv.), THF (0.1 M), 0 °C to rt, 40 min; (b) Lawesson's reagent (1.5 equiv.), pyridine (0.2 equiv.), toluene (0.1 M), 115 °C, 1.5 h; (c) *m*-CPBA (2.2 equiv.), $CH_2Cl_2$ (0.05 M), 0 °C to rt; (d) $Br_2$ (10.0 equiv.), AcOH (0.1 M), $CH_2Cl_2$ (0.1 M), rt, overnight.

ceutical reagents through both metal-catalyzed cross-coupling reactions and light-mediated processes.

## Mechanistic studies

As mentioned above, the excited triplet energies of quinolines **1** and TXs support that quinolines are excited by the photosensitizer TX *via* an EnT process, triggering [2π + 2σ] *ortho*-cycloaddition between quinolines **1** and BCBs **2** to produce cycloadducts **3**. For the subsequent process, we propose a mechanism as follows. The vinylpyridine moiety of a cycloadduct is excited *via* a second EnT process, followed by abstraction of an intramolecular hydrogen atom (HAT) to generate a diradical intermediate, and finally coupling to form the cyclic product **4**.

To confirm the hypothesis of successive EnT-mediated dearomative reactions, we carried out the following experiments, and the details are provided in the ESI.† First, quenching experiments were performed using the typical triplet quenchers $O_2$ atmosphere and (*E*)-stilbene (2.0 equiv.). The former caused a low yield of 9%, and no desired product was detected for the latter but it led to the *E*/*Z* isomerization of (*E*)-stilbene (see the ESI†), indicating that the excited triplet TX is quenched by (*E*)-stilbene. Therefore, the dearomative reactions are triggered by the triplet photosensitizer TX *via* an EnT pathway. On the other hand, the excited reduction potential ($E_{red}(TX^*/TX^{\bullet-})$ = 1.34 V SCE)[21] of the photocatalyst appears to be thermodynamically unfavorable for electron transfer from a quinoline ($E_{ox}$(**1c**) = 1.80 V SCE).[9a]

Monitoring the reaction of **1a** and **2a** by $^1H$ NMR, the intermediate product **3A** and final product **4A** were directly detected at different times (Fig. 2a), and **3A** was isolated and identified as a [2π + 2σ] cycloadduct in 9% yield in a short irradiation time of 10 min. Consistent with previous reports,[12] this cascade transformation is initiated by EnT-mediated dearomative [2π + 2σ] *ortho*-cycloaddition between a BCB and the ben-

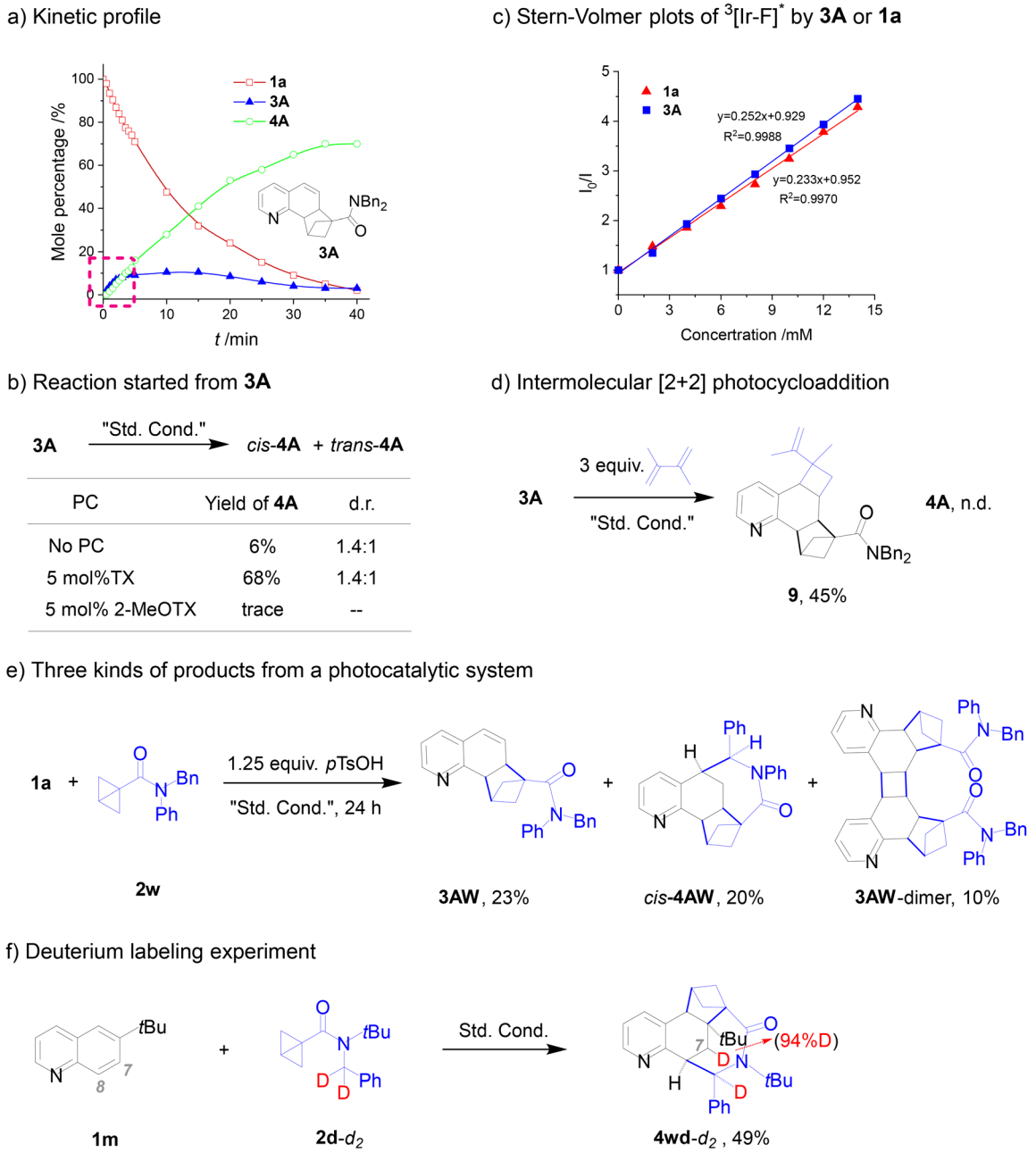


**Fig. 2** Mechanistic investigations. Std. Cond.: standard conditions.

zenoid ring of a quinoline. The kinetic profile shows that **3A** is at a low concentration level, first increasing and then decreasing. In addition, the isolated **3A** can be converted to the target product *cis*/*trans*-**4A** under standard conditions, with the similar reaction result from **1a** and **2a** as starting materials, such as a similar yield (68%) and the same dr value of 1.4 : 1 (Fig. 2b). Under direct irradiation without the photosensitizer, **3A** can also convert to **4A** in a low yield (6%), implying that **4A** could be formed from the triplet **3A** *via* an intersystem crossing (ISC) process of the excited singlet **3A** with low efficiency. Meanwhile, this also rules out another possible pathway, H-abstraction of excited triplet TX ($^3$TX*) from the H-donor as the initial reaction of a cascade cyclization. These observations strongly demonstrate that such [2π + 2σ] cycloadducts are intermediates in the whole conversion.

To clarify the subsequent processes from *ortho*-cycloadduct **3A** to *cis*/*trans*-**4A**, we performed a Stern–Volmer quenching experiment. The result shows that the emission of the excited triplet photocatalyst (here [Ir–F]) is quenched efficiently by **3A** or **1a**, and **3A** seems to be more efficient than **1a** (Fig. 2c). Besides its high reactivity for the intramolecular transformation (from **3A** to **4A**), the excited triplet vinylpyridine **3A** is also reactive in an intermolecular process. For example, 1,2-dimethylbuta-1,3-diene (3.0 equiv.) was added to capture the

 

excited triplet **3A** ($^3$**3A***) to form an intermolecular [2 + 2] cycloaddition product **9** in a fairly high yield of 45% (Fig. 2d).

Based on the following experiment, the triplet energy of the intermediate **3A** is approximately equal to or slightly higher than that of quinoline. Using a low-energy TX, 2-MeOTX (57.8 kcal mol$^{-1}$) as the photosensitizer, only trace products were obtained from the photochemical system of quinoline (**1a**) with **2a** (Table 1, entry 6), and no intermediate **3A** remained. Under the same conditions (2-MeOTX as the photosensitizer), using the intermediate **3A** as the starting material, only trace products were also observed (Fig. 2b). Obviously, the triplet energy of intermediate **3A** is significantly higher than 57.8 kcal mol$^{-1}$ like quinoline. Thus, the EnT process cannot occur between low-energy TX and quinoline, and likewise, intermediate **3A** does not form.

Furthermore, three kinds of products, the intermediate product (**3AW**, 23%), the desired product (**4AW**, 20%) and the [2 + 2] cycloadduct of two **3AW** molecules (**3AW**-dimer, 10%), were obtained from a similar system of **1a**, *N*-phenyl BCB **2w** and *p*-TsOH as an additive (Fig. 2e). This result strongly supports the proposed successive EnT process. Surprisingly, the desired product displays regio- and diastereospecificity, only the 8-to-7 cycloaddition/1,6-HAT/*cis*-coupling product (*cis*-**4AW**) was obtained, and the regio- and diastereospecificity should be from the additive *p*-TsOH, whose mechanism awaits to be elucidated.

Except for the aforementioned **3I** and here **3AW**, no intermediate product **3** was obtained from the reaction mixture when **1** was completely consumed. This implies that in most cases, the conversion from **1** to **3** is a slow process, and that from **3** to **4** is a fast process. In general, the intermolecular [2 + 2] cycloaddition should be slower than the intramolecular 1,6-HAT process. The kinetic profile in Fig. 2a also illustrates clearly the above point, that is, **3A** is always at a low concentration level under the same photosensitization conditions. For the above two cases, the situation is just contrary, that is, the latter conversion (**3** to **4**) is a slow process, in particular, the 1,6-HAT process and/or the cyclization of the diradical Int-2.

The carbon-to-carbon HAT mediated by triplet olefins has been used to construct specific ring systems.[13] The formation of 4-membered[13a–d,f] or 5-membered[13e] rings occurs through intramolecular 1,5- or 1,6-HAT processes, forming 1,4, or 1,5-diradical intermediates. So far, the synthesis of 7-membered rings from a 1,6-HAT process has not been reported.[22] To corroborate that the triplet adducts **3** convert to a 7-membered ring **4** *via* an intramolecular 1,6-HAT process, we performed a deuterium labelling experiment (Fig. 2f). Utilizing double deuterated-benzyl ($PhCD_2$-) BCB **2d**-$d_2$, the dearomative reaction was carried out, affording the desired product **4wd**-$d_2$ in 49% yield in which one deuterium shifted to the C7 position of the "quinoline" (94% deuterium incorporation). This implies that 1,6-HAT indeed occurs in this photochemical reaction. That is, the hydrogen atom at C7 stems from the methylene of the benzyl moiety. This result confirms that the excited triplet **3** can abstract a hydrogen atom from an intramolecular C(sp$^3$)–H bond in the benzyl. As one example, we determined the quantum yield ($\Phi$) for the reaction of **1a** and **2a** under the standard conditions, and the result is 0.91. This value indicates that the dearomative reactions are highly efficient; meanwhile, it rules out a free radical chain reaction.

The aforementioned mechanistic studies have demonstrated the mechanism for successive EnT-enabled photocatalytic reactions, as shown in Scheme 3. The first EnT process from the excited triplet photosensitizer $^3$TX* to a quinoline generates the excited triplet quinoline ($^3$**1***). The electron-rich 8- or 5-position carbon of the triplet quinoline nucleophilically attacks a BCB, forming two regioisomeric 8- and/or 5-diradical intermediates (Int-1), which mainly depends on the substituents (location, size) at the benzenoid ring of the quinoline. The triplet diradical intermediates Int-1 undergo ISC and radical–radical recombination to generate the [2π + 2σ] *ortho*-cycloadduct **3**. The adduct **3** is excited *via* a second

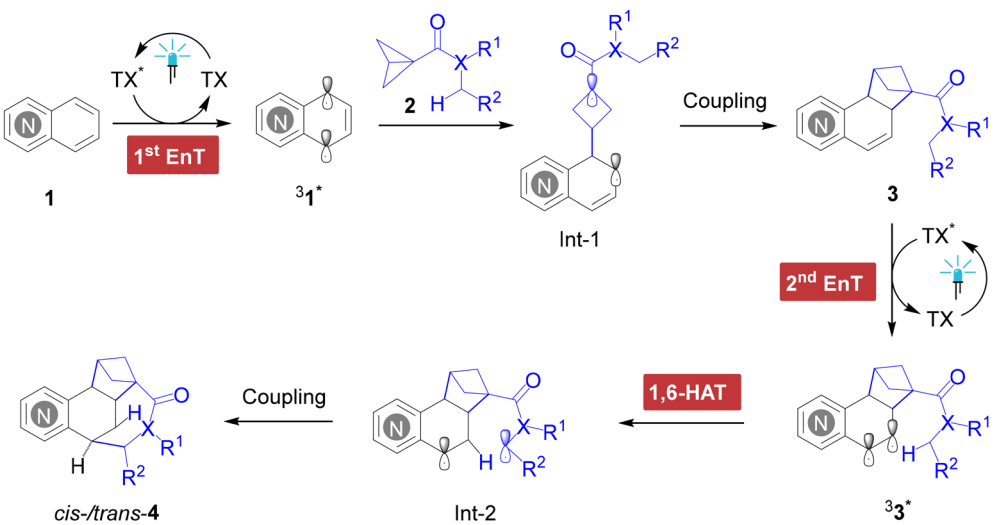


**Scheme 3** Proposed mechanisms.

EnT process from $^3$TX* to its excited triplet state, $^3$**3***, followed by the occurrence of an intramolecular carbon-to-carbon 1,6-HAT, one hydrogen from a remote C(sp$^3$)–H bond at *N*-alkyl to the excited triplet vinylpyridine moiety, forming a triplet 1,7-diradical (Int-2). Finally, the ring closure of Int-2 after undergoing ISC produces the 7-membered ring **4** with certain diastereoselectivity, which is no longer excited by $^3$TX*, as the final product.

The diastereospecificity in the ring closure of 1,7-diradicals (Int-2) was achieved in four systems, **4I**, **4wd**, **4wg** and **4AW**, among which intermediate products **3I** (34%) and **3AW** (23%) were isolated in relatively high yields from the **4I**- and **4AW**-systems after irradiation for a long time, 24 h. As mentioned above, these untransformed **3** imply that the ring closure of the 1,7-diradical is a slow process. Obviously, the slow ring closure of the 1,7-diradical allows it to populate its preferred conformation, followed by coupling to form the target product **4** with diastereoselectivity.

## 3. Conclusions

In summary, we have developed a facile synthetic method for pyridine-fused polycyclic rings with high structural complexity *via* successive EnT-enabled dearomative reactions in a simple photochemical system under mild metal-free catalytic conditions. The reaction mechanism is proposed as a first EnT-mediated dearomative [2π + 2σ] *ortho*-cycloaddition followed by a second EnT-enabled intramolecular carbon-to-carbon 1,6-HAT/cyclization process. The regioselectivity of the [2π + 2σ] cycloaddition depends strongly on the substituent (location, size) of the benzenoid ring of quinoline. The *ortho*-cycloadduct is excited *via* a secondary EnT process, which then triggers the intramolecular 1,6-HAT and finally cyclizes into a 7-membered ring with certain diastereoselectivity, not only enabling the excitable cycloadducts (vinylpyridine) to become photoinert molecules, but also further increasing the molecular complexity. The synthetic utility of this methodology was demonstrated by broad functional group tolerance and compatibility with various bicyclic aza-arenes. This strategy provides an efficient approach for the synthesis of polycyclic architectures and a new route for the comprehensive utilization of the 1,6-HAT of excited olefins to form 1,7-diradical species.

## Author contributions

Yi-Ping Cai: experiments, data curation, formal analysis, writing – original draft; Shi-Ru Chen: experiments; Qin-Hua Song: supervision, administration, analysis, writing – review & editing.

## Data availability

Crystallographic data for *cis*-**4A**, *trans*-**4A**, *cis*-**4f**, *cis*-**4h**, *trans*-**4n** and *cis*-**4wd** have been deposited at the CCDC under 2382179, 2382180, 2382181, 2382182, 2382183 and 2382185,† respectively. Additional data supporting this article have been included as part of the ESI.†

## Conflicts of interest

There are no conflicts to declare.

## Acknowledgements

We are grateful for financial support from the National Natural Science Foundation of China (no. 22074135, 21772188).

## References

1 (*a*) R. Messer, C. A. Fuhrer and R. Häner, Natural Product-Like Libraries Based on Non-Aromatic, Polycyclic Motifs, *Curr. Opin. Chem. Biol.*, 2005, **9**, 259–265; (*b*) W. J. Geldenhuys, S. F. Malan, J. R. Bloomquist, A. P. Marchand and C. J. Van der Schyf, Pharmacology and Structure-Activity Relationships of Bioactive Polycyclic Cage Compounds: A Focus on Pentacycloundecane Derivatives, *Med. Res. Rev.*, 2005, **25**, 21–48; (*c*) C. J. Van der Schyf and W. J. Geldenhuys, Polycyclic Compounds: Ideal Drug Scaffolds for the Design of Multiple Mechanism Drugs?, *Neurotherapeutics*, 2009, **6**, 175–186.

2 R. D. Taylor, M. MacCoss and A. D. G. Lawson, Rings in Drugs, *J. Med. Chem.*, 2014, **57**, 5845–5859.

3 (*a*) S. Felder, S. Dreisigacker, S. Kehraus, E. Neu, G. Bierbaum, P. R. Wright, D. Menche, T. F. Schäberle and G. M. König, Salimabromide: Unexpected Chemistry from the Obligate Marine Myxobacterium Enhygromyxa salina, *Chem. – Eur. J.*, 2013, **19**, 9319–9324; (*b*) F. Feng, J.-H. Liu and S.-X. Zhao, Diterpene Alkaloids from Aconitum Kirinense, *Phytochemistry*, 1998, **49**, 2557–2559; (*c*) J. He, X.-Q. Chen, M.-M. Li, Y. Zhao, G. Xu, X. Cheng, L.-Y. Peng, M.-J. Xie, Y.-T. Zheng, Y.-P. Wang and Q.-S. Zhao, Lycojapodine A, a Novel Alkaloid from Lycopodium Japonicum, *Org. Lett.*, 2009, **11**, 1397–1400; (*d*) J. M. Boente, L. Castedo, A. Cuadros, J. M. Saá, R. Suau, A. Perales, M. Martínez-Ripoll and J. Fayos, *Tetrahedron Lett.*, 1983, **24**, 2029–2030.

4 F. Lovering, J. Bikker and C. Humblet, Escape from Flatland: Increasing Saturation as an Approach to Improving Clinical Success, *J. Med. Chem.*, 2009, **52**, 6752–6756.

5 (*a*) A. Gilbert, The Inter- and Intramolecular Photocycloaddition of Ethylenes to Aromatic Compounds, *Appl. Chem.*, 1980, **52**, 2669–2682; (*b*) J. J. McCullough, Photoadditions of Aromatic Compounds, *Chem. Rev.*, 1987, **87**, 811–860; (*c*) U. Streit and C. G. Bochet, Photoadditions of Aromatic Compounds, *Beilstein J. Org. Chem.*, 2011, **7**, 525–542.

 

6 (*a*) D. Bryce-Smith, Photoaddition and Photoisomerization Reactions of the Benzene Ring, *Pure Appl. Chem.*, 1968, **16**, 47–64; (*b*) A. Gilbert and M. W. bin Samsudin, The Photo-Cycloaddition of Vinyl Acetate to Benzene and its Simple Derivatives: Functionalisation of the Dihydrosemibullvalene Skeleton, *J. Chem. Soc., Perkin Trans. 1*, 1980, 1118–1123; (*c*) P. A. Wender and R. J. Ternansky, Synthetic Studies on Arene-Olepin Cycloadditions-VII: a Three-Step Total Synthesis of (±)-Silphinene, *Tetrahedron Lett.*, 1985, **26**, 2625–2628; (*d*) R. Remy and C. G. Bochet, Arene-Alkene Cycloaddition, *Chem. Rev.*, 2016, **116**, 9816–9849.

7 (*a*) F. Strieth-Kalthoff, M. J. James, M. Teders, L. Pitzer and F. Glorius, Energy Transfer Catalysis Mediated by Visible Light: Principles, Applications, Directions, *Chem. Soc. Rev.*, 2018, **47**, 7190–7202; (*b*) F. Strieth-Kalthoff and F. Glorius, Triplet Energy Transfer Photocatalysis: Unlocking the Next Level, *Chem*, 2020, **6**, 1888–1903; (*c*) A. Palai, P. Rai and B. Maji, Rejuvenation of Dearomative Cycloaddition Reactions via Visible Light Energy Transfer Catalysis, *Chem. Sci.*, 2023, **14**, 12004–12025; (*d*) S. Dutta, J. E. Erchinger, F. Strieth-Kalthoff, R. Kleinmans and F. Glorius, Energy Transfer Photocatalysis: Exciting Modes of Reactivity, *Chem. Soc. Rev.*, 2024, **53**, 1068–1089.

8 (*a*) M. S. Oderinde, S. Jin, T. G. M. Dhar, N. A. Meanwell, A. Mathur and J. Kempson, Advances in the Synthesis of Three-Dimensional Molecular Architectures by Dearomatizing Photocycloadditions, *Tetrahedron*, 2022, **103**, 132087; (*b*) Y.-Z. Cheng, Z. Feng, X. Zhang and S.-L. You, Visible-Light Induced Dearomatization Reactions, *Chem. Soc. Rev.*, 2022, **51**, 2145–2170; (*c*) J. A. Leitch, T. Rogova, F. Duarte and D. J. Dixon, Dearomative Photocatalytic Construction of Bridged 1,3-Diazepanes, *Angew. Chem., Int. Ed.*, 2020, **59**, 4121–4130; (*d*) A. Shimose, S. Ishigaki, Y. Sato, J. Nogami, N. Toriumi, M. Uchiyama, K. Tanaka and Y. Nagashima, Dearomative Construction of 2D/3D Frameworks from Quinolines via Nucleophilic Addition/Borate-Mediated Photocycloaddition, *Angew. Chem., Int. Ed.*, 2024, **63**, e202403461; (*e*) E. Y. K. Tan, A. Dehdari, A. S. Mat Lani, D. A. Pratt and S. Chiba, Dearomative dimerization of quinolines and their skeletal rearrangement to indoles triggered by single-electron transfer, *Chem*, 2024, **10**, 3722–3734.

9 (*a*) J. Ma, S. Chen, P. Bellotti, R. Guo, F. Schäfer, A. Heusler, X. Zhang, C. Daniliuc, M. K. Brown, K. N. Houk and F. Glorius, Photochemical Intermolecular Dearomative Cycloaddition of Bicyclic Azaarenes with Alkenes, *Science*, 2021, **371**, 1338–1345; (*b*) R. Guo, S. Adak, P. Bellotti, X. Gao, W. W. Smith, S. N. Le, J. Ma, K. N. Houk, F. Glorius, S. Chen and M. K. Brown, Photochemical Dearomative Cycloadditions of Quinolines and Alkenes: Scope and Mechanism Studies, *J. Am. Chem. Soc.*, 2022, **144**, 17680–17691.

10 J. Ma, S. Chen, P. Bellotti, T. Wagener, C. Daniliuc, K. N. Houk and F. Glorius, Facile Access to Fused 2D/3D Rings via Intermolecular Cascade Dearomative [2 + 2] Cycloaddition/Rearrangement Reactions of Quinolines with Alkenes, *Nat. Catal.*, 2022, **5**, 405–413.

11 P. Bellotti and F. Glorius, Strain-Release Photocatalysis, *J. Am. Chem. Soc.*, 2023, **145**, 20716–20732.

12 R. Kleinmans, S. Dutta, K. Ozols, H. Shao, F. Schäfer, R. E. Thielemann, H. T. Chan, C. G. Daniliuc, K. N. Houk and F. Glorius, ortho-Selective Dearomative [2π + 2σ] Photocycloadditions of Bicyclic Aza-Arenes, *J. Am. Chem. Soc.*, 2023, **145**, 12324–12332.

13 (*a*) T. Peez, V. Schmalz, K. Harms and U. Koert, Synthesis of Naphthocyclobutenes from α-Naphthyl Acrylates by Visible-Light Energy-Transfer Catalysis, *Org. Lett.*, 2019, **21**, 4365–4369; (*b*) J. Liu, T. Hao, L. Qian, M. Shi and Y. Wei, Construction of Benzocyclobutenes Enabled by Visible-Light-Induced Triplet Biradical Atom Transfer of Olefins, *Angew. Chem., Int. Ed.*, 2022, **61**, e202204515; (*c*) Y. Xiong, J. Großkopf, C. Jandl and T. Bach, Visible Light-Mediated Dearomative Hydrogen Atom Abstraction/Cyclization Cascade of Indoles, *Angew. Chem., Int. Ed.*, 2022, **61**, e202200555; (*d*) M. J. Oddy, D. A. Kusza, R. G. Epton, J. M. Lynam, W. P. Unsworth and W. F. Petersen, Visible-Light-Mediated Energy Transfer Enables the Synthesis of β-Lactams via Intramolecular Hydrogen Atom Transfer, *Angew. Chem., Int. Ed.*, 2022, **61**, e202213086; (*e*) X. Gu, J. Shen, Z. Xu, J. Liu, M. Shi and Y. Wei, Visible-Light-Mediated Activation of Remote C(sp3)-H Bonds by Carbon-Centered Biradical via Intramolecular 1,5- or 1,6- Hydrogen Atom Transfer, *Angew. Chem., Int. Ed.*, 2024, e202409463; (*f*) H. Y. Li, S. Z. Zhang, X. Niu, Q. Y. Meng and X. L. Yang, Visible Light Photocatalyzed Norrish Type II Reaction of Acrylamides for the Synthesis of β-Lactams, *Adv. Synth. Catal.*, 2024, **366**, 1–8.

14 Deposition numbers 2382179 (for *cis*-**4A**), 2382180 (for *trans*-**4A**), 2382181 (for *cis*-**4f**), 2382182 (for *cis*-**4h**), 2382183 (for *trans*-**4n**) and 2382185 (for *cis*-**4wd**)† contain the supplementary crystallographic data for this paper.

15 L. D. Elliott, S. Kayal, M. W. George and K. Booker-Milburn, Rational Design of Triplet Sensitizers for the Transfer of Excited State Photochemistry from UV to Visible, *J. Am. Chem. Soc.*, 2020, **142**, 14947–14956.

16 (*a*) T. Morofuji, S. Nagai, Y. Chitose, M. Abe and N. Kano, Protonation-Enhanced Reactivity of Triplet State in Dearomative Photocycloaddition of Quinolines to Olefins, *Org. Lett.*, 2021, **23**, 6257–6261; (*b*) M. Bhakat, B. Khatua, P. Biswas and J. Guin, Brønsted Acid-Promoted Intermolecular Dearomative Photocycloaddition of Bicyclic Azaarenes with Olefins under Aerobic Conditions, *Org. Lett.*, 2023, **25**, 3089–3093.

17 Y. R. Luo, *Handbook of Bond Dissociation Energies in Organic Compounds*, CRC Press, Boca Raton, 2002.

18 T. G. Denisova and E. T. Denisov, Bimolecular Reactions of Radical Generation Involving Nitrogen-Containing Compounds with Multiple Bonds, *Kinet. Catal.*, 2002, **43**, 1–9.

19 J. Lalevée, X. Allonas and J.-P. Fouassier, N-H and α(C-H) Bond Dissociation Enthalpies of Aliphatic Amines, *J. Am. Chem. Soc.*, 2002, **124**, 9613–9621.

20 D. Wang, L. Désaubry, G. Li, M. Huang and S. Zheng, Recent Advances in the Synthesis of C2-Functionalized Pyridines and Quinolines Using N-Oxide Chemistry, *Adv. Synth. Catal.*, 2020, **363**, 2–39.

21 D.-L. Zhu, R. Xu, Q. Wu, H.-Y. Li, J.-P. Lang and H.-X. Li, Nickel-Catalyzed Sonogashira C(sp)-C(sp2) Coupling through Visible-Light Sensitizatio, *J. Org. Chem.*, 2020, **85**, 9201–9212.

22 (*a*) D. Enders, T. Nguyen and J. Hartmann, Recent Synthetic Strategies to Access Seven-Membered Carbocycles in Natural Product Synthesis, *Synthesis*, 2013, 845–873; (*b*) P. Chen, L. Liang, Y. Zhu, Z. Xing, Z. Jia and T.-P. Loh, Strategies for Constructing Seven-Membered Rings: Applications in Natural Product Synthesis, *Chin. Chem. Lett.*, 2024, **35**, 109229; (*c*) J. Y. Zhang, J. Y. Chen, C. H. Gao, L. Yu, S. F. Ni, W. Tan and F. Shi, Asymmetric (4 (+n) Cycloadditions of Indolyldimethanols for the Synthesis of Enantioenriched Indole-Fused Rings, *Angew. Chem., Int. Ed.*, 2023, **62**, e202305450; (*d*) M. A. Battiste, P. M. Pelphrey and D. L. Wright, The Cycloaddition Strategy for the Synthesis of Natural Products Containing Carbocyclic Seven-Membered Rings, *Chem. – Eur. J.*, 2006, **12**, 3438–3447.

 